

Controlling Plate Vibrations Using Piezoelectric Actuators

Eric T. Falangas, J.A. Dworak, and Shozo Koshigoe

Launch vehicles often experience severe vibration problems during the ascent phase due to intense acoustic fields and mechanically transmitted disturbances. These disturbances are characterized by a large number of resonances over a wide-band frequency spectrum. The payloads inside the launch vehicle must be designed strong enough to withstand these structural vibrations. Passive isolators are used to isolate the payloads from the vibrating structure but this type of isolation has no effect on the acoustic excitations. This study focuses on methods for achieving active damping on plate structures by means of piezoelectric actuators (PZTs). An experiment was conducted using PZT actuators and accelerometers mounted on a rectangular plate with an active damping controller implemented on a 486 computer. Two control design methods were evaluated for this application: the H_∞ method and rate feedback.

Piezoelectric Actuators

Space vehicles do not have to be mechanically robust in order to survive in space. The disturbances in a space environment are relatively small. The space structures do need to be light and compact, in order to meet the weight and volume limitations of launch vehicles. In most cases, the most hostile environment that a space vehicle experiences during its entire lifetime is during launch, and many times the launch phase of a satellite dictates the structural design requirements. If the mechanical loads during launch can be alleviated either passively or via active controls, the satellite can be built to be more lightweight and compact. This reduces launching costs, which run several thousand dollars per pound.

Active damping has been studied for more than ten years. Most studies have focused on controlling the motion of large space structures and on minimizing the disturbances transmitted to the various sensors and optical instruments. This study focuses on control design methods that can be used for driving piezoelectric actuators (PZTs). The PZTs are bonded on the plate structure to remove vibrational energy from the plate and to protect the space payload during launch, either by an active cover that isolates the whole satellite from vibrations, or by protecting sensitive parts of the payload that need to be kept at reduced loads during launch. The goal of this study is to demonstrate vibration damping on a metal plate by means of an experiment. The plate that was used in the experiment resembles some of the panels that cover a space vehicle during launch. Such plates are flat or slightly curved with a thickness of about 1 to 2 mm. Some of

these covers are ejected when the vehicle departs from the earth's atmosphere.

The vibration control experiment was set up at The Aerospace Corporation Dynamics and Control Center. A rectangular plate was used to simulate the dynamic behavior of a satellite panel inside the booster during launch. The purpose of the experiment was to demonstrate the capability of using distributed sensors, actuators, and real-time active digital controls for attenuating vibrations in plate structures. PZTs were selected for providing the local moments on the plate because of their low weight, volume, and cost and their capability to respond at high frequencies (3 to 5 kHz). Models of PZTs bonded or embedded in beams or plates have been developed in [1]-[3]. Control designs at this stage were based on models obtained from experimental data. Accelerometers were used for sensing the motion at various parts of the plate. Accelerometers rather than PZTs or PVDFs were chosen for sensors because of availability. These are small, about one square centimeter in size, and also made out of piezo-electric material. The accelerometers were collocated with the PZTs. Collocation is a good practice, when possible, because the plant becomes minimum phase, positive real, and much easier to control.

Two control methods were considered for this application: rate feedback and H_∞ . Rate feedback uses a low order controller, does not require an accurate plant model, and can easily be implemented. The H_∞ method is more complex and requires a fairly accurate model of the plate modes which are within the control bandwidth. Otherwise, the resulting controller may destabilize the system. From our control analysis, we conclude that the advantages and disadvantages of the two design methods are complementary for this type of problem. The rate feedback was first implemented in the hardware. It provides damping over a

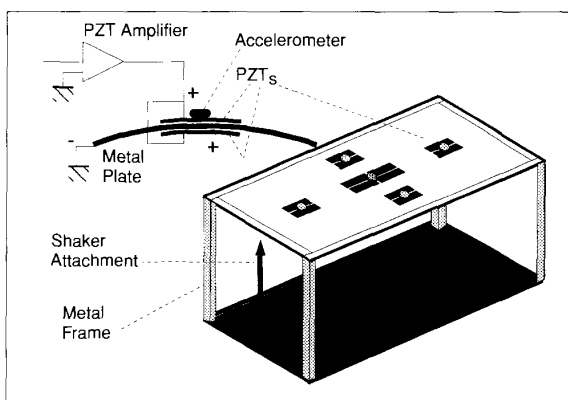


Fig. 1. Experimental apparatus.

The authors are with The Aerospace Corporation, P.O. Box 92957, Los Angeles, CA 90009.

large number of modes, but without a significant attenuation at any specific mode. With H_∞ , the control authority can be focused at specific frequencies, usually the first few modes. The experimental results are described in the results section.

Modeling of Plate with Attached PZTs

The detailed derivation of the plate model with the PZT actuators was presented in [1] by the same authors. In summary, the following second order electromechanical equation describes the dynamic behaviour of the plate modes and their relationship with the forcing functions which are the voltages applied to the PZTs.

$$\rho_p h_p \left(\ddot{\eta}_{qr} + 2\zeta \omega_{qr} \dot{\eta}_{qr} + \omega_{qr}^2 \eta_{qr} \right) = - \left[\frac{(h_p + h_{pzt})}{(1-\nu)} \right] E_{mpzt} d_{31} V_{pzt}(t) \\ \times \int_{x_{FZT} - \frac{\Delta_x}{2}}^{x_{FZT} + \frac{\Delta_x}{2}} \int_{y_{FZT} - \frac{\Delta_y}{2}}^{y_{FZT} + \frac{\Delta_y}{2}} \left(\frac{\partial^2}{\partial x^2} + \frac{\partial^2}{\partial y^2} \right) \Phi_{qp}(x,y) dx dy$$

where ω_{qr} are the plate mode frequencies obtained from the following equations:

$$\omega_{qr} = \sqrt{\frac{D}{\rho_p h_p}} \left[\left(\frac{q\pi}{a} \right)^2 + \left(\frac{r\pi}{b} \right)^2 \right]$$

where the stiffness

$$D = \frac{h_p^3 E_{mpl}}{12(1-\nu^2)}$$

and ρ_p is the plate density in kilograms per square meter, h_p is the plate thickness in meters. d_{31} is the piezoelectric actuator strain constant in meters per volt, $V_{pzt}(t)$ is the voltage applied across the PZT in volts, ν is the Poisson ratio for the plate, E_{mpl} is the Young's modulus for the plate in newtons per square meter, x_{pzt}, y_{pzt} is the location of the center of a PZT on the plate, Δ_x, Δ_y , are the dimensions of a PZT along x and y , h_{pzt} is the PZT thickness in meters, E_{mpzt} is the Young's modulus for the PZT (newtons per square meter), $\eta_{qr}(t)$ is the generalized displacement of plate mode (q,r) in meters, $\Phi_{qr}(\xi)$ is the mode shape or eigenvector of plate mode (q,r) at a location (ξ) on the plate, which is

$$\Phi_{qr}(\xi) = \frac{2}{\sqrt{ab}} \sin\left(\frac{q\pi}{a}x\right) \sin\left(\frac{r\pi}{b}y\right)$$

The subscripts q and r are the plate mode indices along the x and the y directions, respectively: i.e., $q=1,2,3,\dots$ and $r=1,2,3,\dots$

Experimental Apparatus

PZTs are piezoelectric ceramic materials that can be distorted by the application of an electric field. The piezoelectric elements

used in this experiment are shaped in the form of thin plates approximately 2×5 cm in area and 0.2 mm thickness. The piezoceramic material is not effective before it becomes poled. The material must be poled during manufacturing by the application of a large electric field, usually at high temperature. During application as an actuator, the PZT should be operated well below the depoling field which is approximately 750 V/mm thickness, typically 150 V in our application.

The piezoelectric actuator plates can be bonded on the surface of a flat or slightly curved plate structure. The application of an electric field along the polarization direction forces it to expand along the directions perpendicular to the electric field, producing a local strain on the plate surface. On the other hand, if the electric field is opposite of the polarization direction, the PZT will contract in the direction perpendicular to the electric field. This expansion or contraction of the PZT element bonded on a plate generates a local moment on the plate surface. The amount of the local moment is proportional to the applied voltage. If the applied voltage is kept at a low level (well below the depoling level), the relationship between the local moment and PZT voltage is linear.

The experimental apparatus is shown in Fig. 1. It consists of a 0.5×0.6 m rectangular aluminum plate 1-mm thickness, mounted on a frame and supported by a metal beam structure. There are five PZT patch pairs which are bonded on the plate. Each pair consists of a top patch which is bonded on the top side of the plate, and an identical patch bonded on the bottom side of the plate, directly below the top patch. The two patches sandwich the plate, and they both constitute one actuator (see top left of Fig. 1). A conductive adhesive is used to bond the patches on the plate. One patch pair (actuator) is located at the center of the rectangular plate, and four other pairs between the center and four sides.

Each patch consists of several PZT elements connected in parallel for more effectiveness. The double patch action (one above and one below the plate) generates a pure local moment on the plate without a stretch. The PZT pairs are connected in such a way that when the patch above the plate stretches, the corresponding one below the plate shrinks. Each pair of PZT patches (one above and one directly below the plate) are connected in parallel to the output of a power amplifier so both receive equal voltage. There are five amplifiers, one for each actuator (patch pair). The amplifiers supply the PZTs with a feedback voltage which can be as high as ± 150 V. In Fig. 2, when

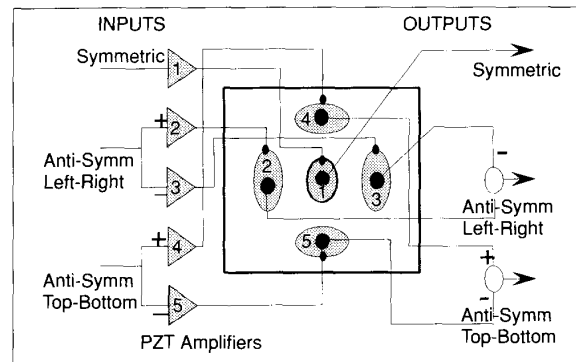
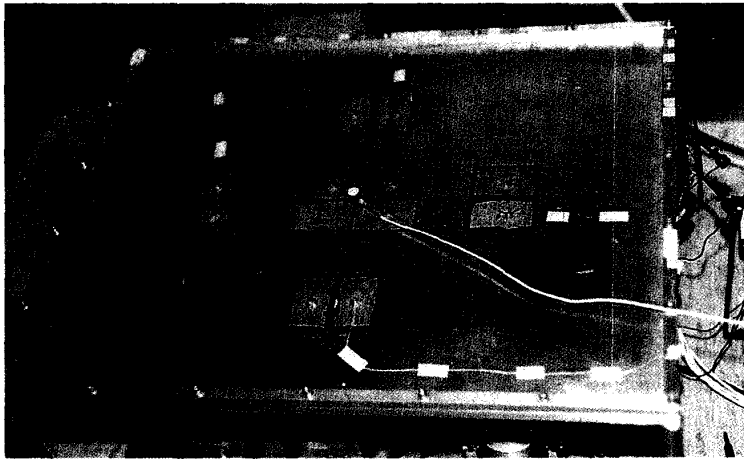


Fig. 2. Cross-coupled control approach.

a small voltage (0 to ± 3 V) from the D/A converter is applied at the input of the amplifier, the amplifier generates the voltage required to generate sufficient local moment for bending the plate and damping out the mechanical vibrations. In the experiment, the vibrations are produced by a shaker that is attached to the plate and driven by a noise generator. The shaker generates random disturbances that excite the plate modes. The bandwidth of the noise generator is adjusted to match the actual disturbances obtained from launch measurements.



Five accelerometers are placed on the top and center of each PZT actuator. They are used to sense the acceleration of the plate at the center of the patches and to provide measurement signals into the control system. The accelerometers which are also made out of piezoelectric material, require further amplification before driving the A/D converter. The control system is implemented in a 486 computer using C++. The computer interfaces with the five accelerometer amplifiers via the A/D converters on one side, and on the other side with the five PZT amplifiers via the D/A converters and the analog low pass filters. The digital control algorithm in the computer generates the feedback signals that drive the five PZT amplifiers based on the signals read from the five accelerometers.

Control System

The control system generates local moments on the plate in a direction that opposes the plate motion. In essence, it actively enhances the damping of the plate modes. There are many actuator/sensor combinations that one may choose to close the loops between the accelerometers and the PZTs (control configurations). There are also different control system design methods that can be used to synthesize a controller that actively reduces the excitation of the plate modes in response to acoustic or mechanical noise.

Control Configurations

Two control configurations were considered in this experiment: a) a localized feedback approach, described in [1], where each accelerometer drives only the collocated PZT and b) a cross-coupled approach. In both configurations the accelerometers are collocated with the PZT actuators. In this article we will

present only the analysis and results obtained from the cross-coupled configuration. The actuator/sensor collocation guarantees that the system is positive real, at least for the lower frequency modes. It is also minimum phase which is a good property for applying LQG or H_∞ design methods. This guarantee does not apply to higher frequency modes, because the collocation principle does not apply to modes of wavelength comparable to the size of the PZT actuator. In addition, computational delays at high frequencies can drive some higher frequency modes unstable.

The cross-coupled control approach is shown in Fig. 2. It consists of three control loops. The five collocated actuator and sensor pairs are combined in an attempt to decouple mainly the first three plate modes, the first symmetric, the first anti-symmetric in the left/right direction, and the first anti-symmetric in the top/bottom direction. Each actuator (pair of patches) is driven by an amplifier that can supply up to 150 V. The five accelerometers sense the plate motion in the middle of each patch. The cross-coupled configuration in Fig. 2 has three inputs and three outputs. The input to each amplifier is received via a transformation that decouples the excitation of the first three modes. The amplifier inputs are coupled in such a way so that: system input #1 excites mainly the first mode and also other symmetric modes, system input #2 excites the left/right anti-symmetric modes, and system input #3 excites the top/bottom anti-symmetric modes.

A similar transformation is also performed at the sensors, in order to combine the five accelerometer signals into three system outputs. In fact, the output transformation is equal to the transpose of the input transformation, and they are shown pictorially in Fig. 2. The output transformation decouples the sensing of the plate modes, so that: system output #1 senses mainly the first and all the symmetric modes, but not the anti-symmetric modes; system output #2 senses mainly the left/right anti-symmetric mode plus other high frequency anti-symmetric modes from left to right; and similarly, system output #3 senses the top/bottom anti-symmetric modes. The cross-coupled configuration attempts to decouple the plate modes and transform the system into a diagonally dominant one, by separating the plate modes into three control loops. Ideally, one would expect all the symmetric modes to be present in the first loop, the left/right anti-symmetric modes to be in the second loop, and the top/bottom anti-symmetric modes to be in the third loop. In the actual experiment however, this is not exactly the case. There is some small interaction between the loops due to the lack of symmetry caused by differences between the PZTs. Although all PZTs are made from the same ceramic material, bonding them on the metal plate with identical effectiveness is not easy. The strain generated from each PZT strongly depends on the amount of conductive glue applied between the plate and the PZTs during bonding, and the effectiveness of the glue at the time of bonding. But for all practical purposes diagonal dominance is achieved. The diagonalization also helps in control design, because fewer modes appear in each loop. It reduces the order and complexity of the control system because each control loop focuses on different modes.

There are other practical advantages for separating the multiloop design into three SISO designs: a) frequency response characterization of the system can be obtained from experiments, the characterization data can be used to curve fit accurate transfer functions of the plant dynamics (between PZT voltage to accelerometer voltage) for the purpose of designing more efficient controllers, and b) the controller implementation can be accomplished in steps, rather than incorporating the complete design at once, making it easier to locate possible hardware problems.

Control Design Methods

Two control methods were considered for closing the loops between the accelerometers and the piezoelectric actuators: a) rate feedback by integrating the accelerometer signal, and b) dynamic feedback obtained via the H_∞ design methodology.

Rate Feedback

The rate feedback design approach is simple and easy to implement. The idea is to integrate the accelerometer signal that senses the motion of the plate over the PZT actuator, amplify it, and feed it back to the PZT. The integration process shifts the phase of the accelerometer measurement by 90° to provide a feedback that is proportional to the local rate. This effectively increases the damping in all modes which are controllable and observable (see Fig. 3).

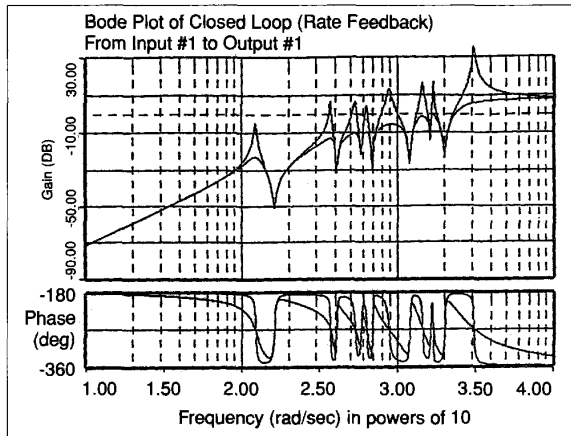


Fig. 3. Open-loop versus closed-loop response via rate feedback.

Fig. 4(a) shows the Nichol's plot analysis of the center loop system with rate feedback. The direction of the circular resonances indicate that for the first several modes the system behaves like a positive real system, and it appears to be stable regardless of the value of the loop gain. In fact, increasing the gain seems to improve the closed-loop modal damping in all the modes; see Fig. 3. This apparent stability robustness and overall mode attenuation with rate feedback predicted in the analysis, is of course not true at all frequencies. Active damping ceases at high frequencies, even causing instabilities in high frequency modes when the loop gain is increased for the following reasons:

- 1) The PZT actuator performance deteriorates at frequencies above 3-5 kHz and introduces phase lag.
- 2) Computational delays introduce phase lag which increases as the frequency approaches the Nyquist frequency. This dete-

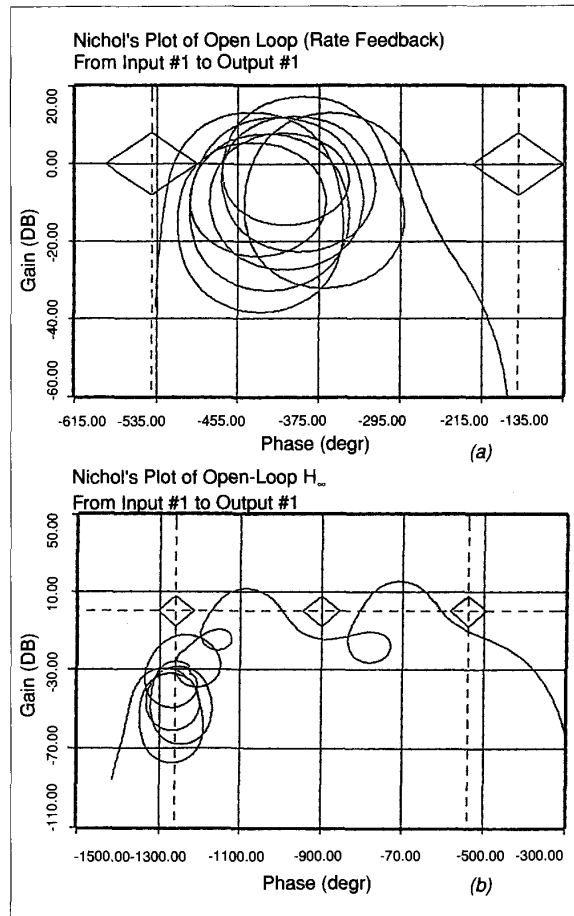


Fig. 4. Nichols plots: (a) rate feedback, (b) H_∞ control.

riorates the phase margin at high frequencies and may drive some high frequency modes unstable, if left unattenuated. Reducing the loop gain prevents high-frequency mode instabilities, but it limits the overall system's performance (less damping).

3) The sensor is not exactly collocated with the actuator. The actuator patch is spread over a larger area while the accelerometer measurement is at a point. This lack of perfect collocation does not affect the low frequencies, but as the mode wavelength becomes shorter and comparable to the size of the patch, part of the patch may be moving in one direction while part of the patch moves in the opposite direction. This effect can drive some high frequency modes unstable, if these modes are left unattenuated in the control loop.

The ground rule for rate feedback is that the higher the gain the better the damping, but there is a limit. You cannot increase the gain too much before it destabilizes one of the high frequency modes. The control design with rate feedback is relatively simple. We used the following approach:

- 1) The loop was closed by integrating the accelerometer measurement, thereby providing rate feedback. A first-order lag filter $5/(s+5)$ was used instead of a pure integrator because the accelerometer signal has a small dc bias which otherwise causes

control voltage saturation. A small loop gain was first used, and it was increased until one of the high frequency modes approached instability. The highest gain value that resulted in stable response was used in the design.

2) The first order lag was replaced with a second order compensator. The new compensator altered the phase characteristics at some of the high frequency problem modes. It essentially performed like the integrator at low frequencies but allowed us to increase the gain a little higher before high mode instabilities occurred.

The following factors also limit the performance of the rate feedback controllers:

1) The rate feedback controller does not discriminate between modes. It spreads the control authority to all the modes, even to modes that may not require attenuation. This approach demands more powerful actuators.

2) Introducing roll-off filters is not very practical in this situation because there is a large population of modes widely spread over the entire frequency range, without a frequency gap between the modes wide enough to place a roll-off filter. Placing the cutoff frequency of a roll-off filter within a largely populated region, causes some of the modes to become unstable.

3) Another limiting factor on the size of the rate feedback gain is the magnitude of the external disturbances. The shaker provides a random excitation to the plate. The PZT actuator is attempting to counteract the disturbance, and the stronger the excitation on the plate the higher is the demanded PZT voltage. If the voltage approaches saturation levels, the PZT actuator becomes ineffective and the loop gain must be lowered to avoid voltage saturation. Lowering the gain, also reduces attenuation performance.

H_∞ Design Method

Unlike the rate feedback which damps out several modes with a simple integrator, the H_∞ controller is dynamic, and its order is comparable to the plant model. The H_∞ optimization algorithm of Doyle *et al.* was applied in this study [5]-[7]. The unreduced controller typically consists of one second-order resonance for each plate mode that must be attenuated. Instead of resisting the motion at all frequencies, as rate feedback does, the H_∞ controller behaves like counter resonances which eliminate the effects of the mechanical resonances at the system's output. This design, unlike the rate feedback, requires knowledge of the plant dynamics. This information is used by the H_∞ controller to focus the control authority at specific modes which perhaps exceed the launch environment noise specifications, instead of spreading the control over a wide frequency range.

H_∞ Synthesis Model

The H_∞ design is based on a *synthesis model*. Before the H_∞ optimization algorithm can be applied with meaningful results, the designer must specify a synthesis model (SM). The SM consists of the plant dynamics, the control inputs and disturbance inputs, the measurements, and the criteria outputs. A typical synthesis model is shown in Fig. 5. It not only consists of the plant dynamics specified in terms of control inputs and output measurements, but also includes additional inputs and output vectors to represent disturbance inputs and output criteria to be minimized. The disturbances describe how the noise corrupts the

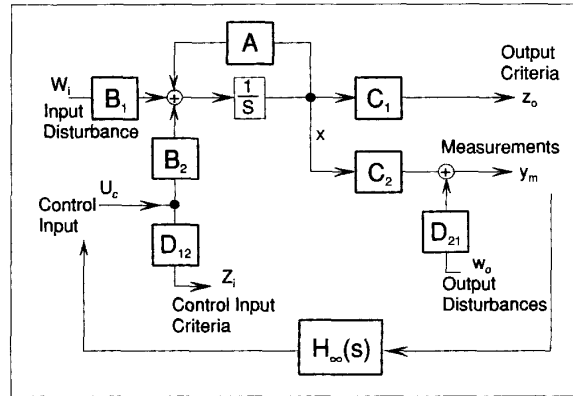


Fig. 5. H_∞ synthesis model.

plant both at the input and at the sensors. The criterion vector consists of a combination of variables (state variables and control inputs), which must be minimized by the H_∞ algorithm in the presence of disturbances. The SM for H_∞ consists of nine matrices. It has two types of inputs: a control input vector (u_c) and a disturbance input (w). The disturbance consists of two parts: (a) an input disturbance vector (w_i) which directly excites the state-vector, and (b) an output disturbance (w_o) that represents the noise at the sensor or plant uncertainty. The SM also has two sets of outputs: a) a measurements vector (y_m), and b) the criterion output vector (z). The criterion consists of two parts: a) the criterion (z_o) which is a linear combination of the states, and b) the (z_i) part that acts like a penalty on the control inputs.

Some of the SM matrices are part of the plant dynamics, while other matrices are design parameters. The matrices which are part of the plant dynamics are: the state-transition matrix A , the control input matrix B_2 , the input disturbance matrix B_1 , and the measurements output matrix C_2 . The matrices C_1 , D_{12} , and D_{21} are not necessarily part of the physical plant model (although C_1 may be). These matrices are selected as design parameters for stability versus performance trade-off. For example, C_1 presents a set of criteria variables in the H_∞ optimization, D_{12} weights the control inputs in the optimization process and bounds the control system's bandwidth, and D_{21} reflects the effect of noise, uncertain dynamics, or sensor errors in the measurements. The matrices D_{12} and D_{21} must be square, full rank, and diagonal for meaningful interpretation.

The control system design goal is to close the loop between the measurements y_m and the control inputs u_c via a dynamic controller, so that the infinity norm of the sensitivity transfer function between the disturbances (w) and the output criterion (z) is minimized in the closed-loop. This minimization results in a system that is less vulnerable to disturbances. In our plate model, this sensitivity minimization is accomplished by using the PZT actuators to actively damp out the plate vibrations. Note however, that this sensitivity minimization occurs only in the plant modes which have been included in the SM. There is no guarantee that the other modes will be damped out; in fact they might even go unstable. In order to avoid this spillover effect, we filter out the high frequency modes in the feedback loop by means of loop-shaping techniques.

Decoupled System

Our design goal is to control the plate modes by means of three decoupled SISO control loops. The first loop consists of the modes which are symmetric about the center of the plate, the system input activates the center PZT actuator and the output measures the acceleration at the center of the patch. The input to the second loop drives the left and right actuators differentially by applying equal and opposite voltages at the left and right PZTs. The output of the second loop reads the left and right accelerometers differentially (i.e., left-right). Similarly, the input to the third loop drives the top and bottom actuators differentially, and the output from the third loop reads the top and bottom accelerometers differentially. This control configuration decouples the plate modes into three SISO systems. The control design approach for the three cases is similar, so only the center loop design will be discussed.

H_∞ Design Process

In order to apply the H_∞ method, a reduced size model is required consisting mainly of the modes to be attenuated. For the center patch loop, for example, the design model $G(s)$ contains only the first three symmetric modes. Although attenuation is intended only on the first two symmetric modes, the third mode is also included in the SM because it is near the system bandwidth. The H_∞ method guarantees stabilization to all the modes which have been included in the synthesis model; otherwise, if the third mode is not included it becomes unstable.

Loop Shaping before H_∞

Loop shaping is used to specify closed-loop objectives in terms of requirements on the open-loop characteristics. Simplistically, by selecting a controller with a high open-loop gain at the mode frequencies that we want to control and a low gain at high frequencies, good closed-loop performance and robustness can be achieved against unmodeled high frequency dynamics. It is possible to shape the open-loop characteristics of the nominal design model $G(s)$ by pre- and post-filter multiplication with compensators, so that the open-loop system exhibits the desired properties (Fig. 6(a)).

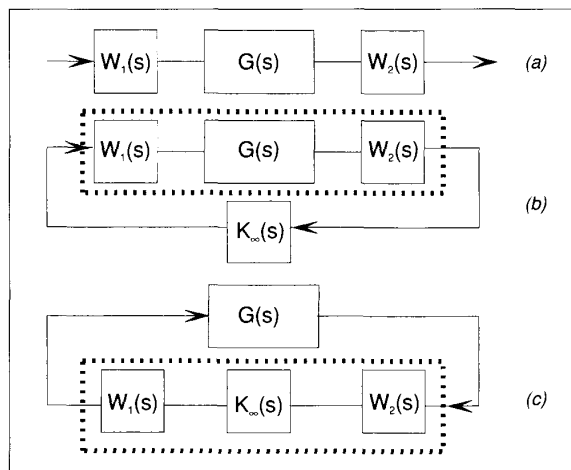


Fig. 6. Loop shaping design: (a) augmented plant, (b) controller for the augmented plant, (c) augmented controller for the original plant.

The shaping filters $W_i(s)$ are combined in series with the reduced order design plant $G(s)$ to form the augmented synthesis model $G_s(s) = W_i(s) G(s)$ (Fig. 6(a)). The H_∞ algorithm is then applied on the augmented plant $G_s(s)$ to obtain an H_∞ controller $K(s)$ (Fig. 6(b)) that stabilizes this plant and meets certain design requirements which were reflected in the shaping filters $W_i(s)$. The final feedback controller $K(s)$ for the original plant $G(s)$ is constructed by combining the controller $K(s)$ with the shaping filters $W_i(s)$ so that $K(s) = W_i(s) K(s)$ (Fig. 6(c)).

Shaping Filters $W_i(s)$

The question arises, how do we choose the shaping filters to reflect the performance and robustness requirements of the closed loop system in the H_∞ synthesis model? This requires some experimentation in the beginning. The main requirement for the controller is to provide damping for the first two symmetric modes. Higher frequency modes do not have to be controlled but they must be protected from going unstable. This requirement is reflected in the synthesis model by placing a roll-off shaping filter with a cutoff frequency a little higher than the second mode (350 rad/s). We used a first order low pass $W_1(s) = 350/(s+350)$.

A low frequency requirement also is needed in the control system design. The control system must not have an integrating action but the controller gain should be kept small at low frequencies. The reason for this requirement is because the accelerometer signal has a small dc bias that would saturate the controller if the controller had an integrator in the loop. This dc bias causes a constant plate deflection when the loop is closed. For this reason the controller gain must be as small as possible at dc. This requirement is introduced in the design by adding a second shaping filter in the synthesis model, a high-pass filter for preventing the H_∞ controller to respond at dc. The high pass shaping filter transfer function is $W_2(s) = s/(s+15)$.

The two shaping filters were included in our first design attempt. A controller was obtained that attenuates the first two modes, but this controller destabilizes a higher frequency mode which was not included in the H_∞ synthesis model, at 870 rad/s. Experimental data show there is a cluster of modes near that frequency. We obviously do not want to damp out all these modes around that frequency, we simply want to filter them out so the control system will not respond at frequencies around 870 rad/s. A notch filter with a notch at 870 rad/s was added to the previous two shaping filters to provide more attenuation at that frequency.

The three shaping filters are now combined with the design plant $G(s)$ to form the augmented synthesis plant $G_s(s)$. Another modification was made to the design model which led to better results. The original design model was based on accelerometer measurements, it has an " s^2 " in the numerator because of the accelerometer. This model was replaced with a velocity transfer function model which has an " s " in the numerator instead of an " s^2 ." The shaping filters remained the same. The final controller was modified at the end of the design by removing an " s " from its numerator, to match the original plant with acceleration measurement. The augmented shaped plant transfer function becomes

$$G_s(s) = \left[\frac{s}{(s+15)} \right] * \left[\frac{350}{(s+350)} \right] * \left[\frac{s^2+105s+866^2}{s^2+600s+608^2} \right]$$

$$* \left[\frac{s}{(s^2+2\zeta_{p1}\omega_{p1}s+\omega_{p1}^2)} \right] * \left[\frac{(s^2+2\zeta_{z2}\omega_{z2}s+\omega_{z2}^2)}{(s^2+2\zeta_{p2}\omega_{p2}s+\omega_{p2}^2)} \right] * \left[\frac{(s^2+2\zeta_{z3}\omega_{z3}s+\omega_{z3}^2)}{(s^2+2\zeta_{p3}\omega_{p3}s+\omega_{p3}^2)} \right]$$

The H_∞ synthesis algorithm is applied on the augmented shaped plant $G_s(s)$ to obtain a controller $K(s)$ for $G_s(s)$, as in Fig. 6(b). The shaping filters are then combined with $K(s)$ to form an augmented controller for the original plant $G(s)$ (Fig. 6(c)). The augmented controller for the center patch loop system was 15th order. It was reduced in size to a 10th order by using the *internal balancing model reduction* method [4], [6]. A similar design process was repeated for the other two loops, the left/right anti-symmetric model, and the top/bottom anti-symmetric model.

Analytic and Experimental Results

The analysis results presented in this section are based on three decoupled models that were obtained from the experiment via a frequency characterization process. The modal decoupling configuration (Fig. 2) assures that the system is almost diagonal with minimal coupling between the three loops. Three transfer function models were obtained. The first one, called the center patch loop, was obtained from the frequency response between the center PZT actuator voltage and the voltage from the center accelerometer. The second one, known as the "left-right" anti-symmetric loop, was obtained by exciting the left and right actuators with equal and opposite voltages and reading the difference between the left and right accelerometer voltages. Similarly, the "top-bottom" anti-symmetric loop, was obtained by exciting the top and bottom actuators with equal and opposite voltages, and reading the difference between the top and bottom accelerometers.

Fig. 4 compares the difference between the two control designs. Fig. 4(a) shows the Nichol's plot of the rate feedback system, and Fig. 4(b) is the Nichol's plot for the H_∞ design. Every loop represents a mode resonance. The computational and other delays have not been included in the models. In the rate feedback case (Fig. 4(a)), the loop gain is large for all modes (they are all above the 0-dB line). It is obvious that when computational and other delays are introduced in the system, the high-frequency resonances will shift to the left, and some of them will encircle the critical point becoming unstable. In the H_∞ design (Fig. 4(b)), however, only the first two modes are exceeding the 0 dB line. These are the two design modes that require high loop gain to achieve active damping. Computational delays do not effect the first two modes, because they are significantly lower than the Nyquist frequency. The high frequency modes; however, they are attenuated below -10 dB. The attenuation guarantees that these modes will be stable even with transport delays.

Fig. 7 demonstrates active damping results measured from the experiment. The three loops were individually closed by means of three H_∞ controllers, and then all three together via a multiloop controller. The plate modes were excited with taps at arbitrary points on the plate. The overlay curves correspond to the open-loop versus the closed-loop frequency responses of the plate. Obviously the closed-loop responses exhibit better damping and lower magnitudes at the resonances than the open-loop re-

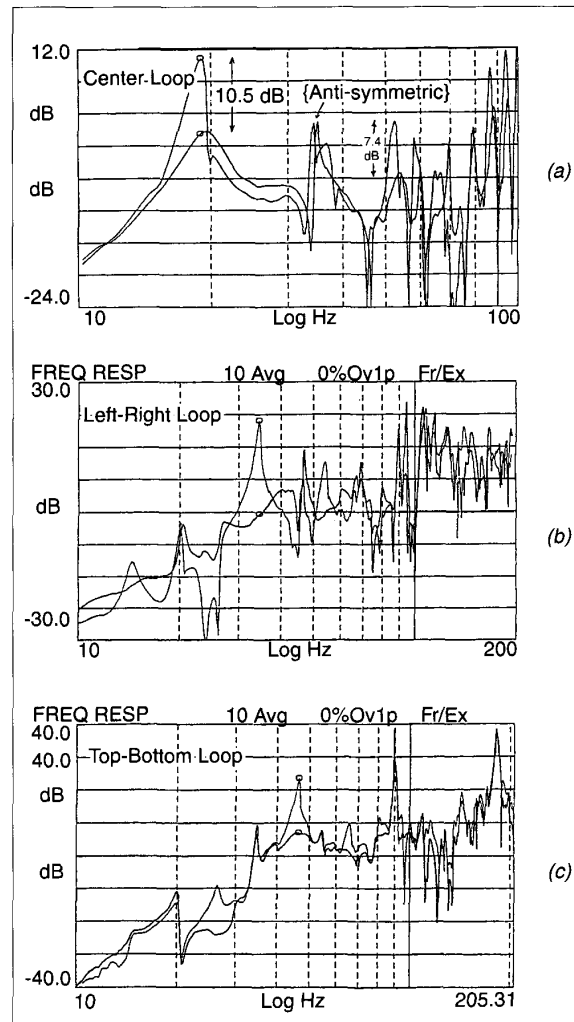


Fig. 7. Experimental results when the three loops are closed independently, open-loop versus closed-loop frequency responses.

sponses. Fig. 7(a) corresponds to the center loop. It shows that active damping was achieved in the first two symmetric modes. The first symmetric mode at 19 Hz was attenuated by 10.5 dB and the second symmetric mode at 55 Hz was attenuated by 7.4 dB. Fig. 7(b) corresponds to the "left-right" loop. The emphasis here was placed on the first left/right anti-symmetric mode (34 Hz). It shows that this mode was attenuated approximately 17 dB. Similarly, Fig. 7(c) corresponds to the "top-bottom" loop. The first top/bottom anti-symmetric mode (46 Hz) was targeted and was attenuated approximately 17 dB.

Robust Control Design Methods

The motivation for this work was to demonstrate practical applications of robust control design methods in vibro-acoustic control problems. These fairly new design techniques were selected for this type of application because of their capability to direct the control at specific problem frequencies by means of

loop-shaping. In a real launch environment these problem frequencies may be structural resonances of a satellite inside a launch vehicle, or acoustic disturbances exciting the structure, or both. The performance of the H_∞ controller was significantly superior to the rate feedback. The difference is clearly visible by just tapping on the plate with your finger. The only advantages of rate feedback are its simplicity and the overall mode attenuation, but we discovered that passive visco-elastic materials can provide even better overall mode attenuation than rate feedback. These are visco-elastic patches that can be bonded at various places on the surface of the plate. They are very effective in attenuating high frequency modes but not as good at lower frequencies. Therefore, passive visco-elastic damping and H_∞ active control at selected low frequency modes, make a good combination together. It is also much easier to design active controllers for the low frequency modes when the high frequency modes are attenuated passively, (less roll-off and notch filtering necessary). At the present time our vibro-acoustic control research has shifted in two directions: a) active vibration isolation systems [8], and b) acoustic control inside cavities [9].

References

- [1] J.A. Dworak, E.T. Falangas, S. Koshigoe, and G.T. Tseng, "Vibro-acoustic control using PZT actuators," presented at the 3rd Int. Conf. Adaptive Structures in Nov. 92, San Diego, CA.
- [2] E.F. Crawley, J. de Luis, N.W. Hagood, and E.H. Anderson, "Development of piezoelectric technology for application in control of intelligent structures," in *Proc. 1988 Amer. Control Conf.*, 1988, vol 3, pp. 1890-1896.
- [3] E.F. Crawley and J. de Luis, "Use of piezoelectric actuators as elements of intelligent structures," *AIAA J.*, vol. 25, no. 10, pp. 1373-1385.
- [4] B.C. Moore, "Principal components analysis in linear systems: Controllability, observability, and model reduction," *IEEE Trans. Auto. Control*, vol. AC-26, no. 1, Feb. 1981.
- [5] J.C. Doyle, K. Glover, P.P. Khargonekar, and B.A. Francis, "State-space solutions to standard H_2 and H_∞ control problems," *IEEE Trans. Auto. Control*, vol. 34, no. 8, Aug. 1989.
- [6] R.L. Dailey, "Lecture notes for the workshop on H_∞ and μ methods for robust control," presented at the 1990 Amer. Control Conf., San Diego, CA, 1990.
- [7] M.G. Safonov, D.J.N. Limebeer, and R.Y. Chiang, "Simplifying the H_∞ theory via loop-shifting, matrix-pencil and descriptor concepts," *Int. J. Control*, vol. 50, no. 6, 1989.
- [8] E.T. Falangas, "A vibration isolation system that uses active PZT brackets," presented at the 1994 Amer. Control Conf., Baltimore, MD, 1994.
- [9] S. Koshigoe, J.T. Gillis, and E.T. Falangas, "A new approach for active control of sound transmission through an elastic plate backed by a rectangular cavity," *J. Acoustics Soc. Amer.*, Aug. 1993.



Eric T. Falangas was born in Athens, Greece. He received the B.Sc. degree in electrical engineering from the University of London, England, in 1972, and the M.Sc. degree in control systems from the University of Manchester (UMIST), Control Systems Center, in Manchester, England. He was employed by Rockwell International from 1977 to 1989, where he supported several aerospace programs such as the Space Shuttle, Space Station proposal, and other SDI programs. While he was at Rockwell he also completed additional 43 units in post-graduate work at the University of Southern California, in flight dynamics and control systems. He is currently employed at the Aerospace Corporation, Pointing and Control Office. His interests are in control theory and applications, flight control, spacecraft attitude control, and vibration isolation systems.



Joe A. Dworak received the B.S. degree in mechanical engineering and the M.S. degree in nuclear engineering from the University of Missouri. After a three year period of employment as a Research Scientist with Batelle Columbus Laboratories, he began the Ph.D. program in mechanical engineering at The Ohio State University, specializing in systems modeling and applied control. After graduation he accepted a position in automated manufacturing and process controls with the General Electric Company. He is currently Manager of the Controls, Sensors, and Electronics Section of the Aerospace Corporation, responsible for spacecraft and launch vehicle attitude determination and control components.



Shozo Koshigoe received the B.S. degree in physics from Ehime University in 1973, the M.S. degree in physics from The University of Texas in 1979, and the Ph.D. degree in physics from Purdue University in 1983. He worked at Sansui Electric Co. from 1973 to 1976 as an Acoustic Engineer. From 1983 to 1989, at the Naval Weapons Center, he worked on combustion instability in solid rocket motors and development of stability theory for noncircular jets. He is currently employed by the Aerospace Corporation and his main work involves development of an active noise control technology for future launch vehicles.